Nucleic Acids Research, 1997, Vol. 25, No. 22 **4551–4556**

Structural studies on tRNA acceptor stem microhelices: exchange of the discriminator base A73 for G in human $tRNA^{Leu}$ switches the acceptor specificity from leucine to serine possibly by decreasing the stability of the terminal G1–C72 base pair

Armin U. Metzger, Martha Heckl[1], Dieter Willbold, Kristin Breitschopf[1,+], Uttam L. RajBhandary[2], Paul Rösch* and Hans J. Gross[1]

Lehrstuhl für Biopolymere, Universität Bayreuth, D-95440 Bayreuth, Germany, [1]Institut für Biochemie, Bayerische Julius-Maximilians-Universität, Biozentrum, Am Hubland, D-97074 Würzburg, Germany and [2]Department of Biology, Massachusetts Institute of Technology, Cambridge, MA, USA

Received August 1, 1997; Accepted September 29, 1997

ABSTRACT

Correct recognition of transfer RNAs (tRNAs) by aminoacyl-tRNA synthetases (aaRS) is crucial to the maintenance of translational fidelity. The discriminator base A73 in human $tRNA^{Leu}$ is critical for its specific recognition by the aaRS. Exchanging A73 for G abolishes leucine acceptance and converts it into a serine acceptor *in vitro*. Two RNA microhelices of 24 nt length that correspond to the $tRNA^{Leu}$ acceptor stem and differ only in the discriminator base were synthesized: a wild-type $tRNA^{Leu}$ microhelix, where nt 21 corresponds to the discriminator base position 73, and an A21G mutant microhelix. To investigate whether different identities of both tRNAs are caused by conformational differences, NMR and UV melting experiments were performed on both microhelices. Two-dimentional NOESY spectra showed both microhelices to exhibit the same overall conformation at their 3′-CCA ends. Thermodynamic analysis and melting behaviour of the base-paired imino protons observed by NMR spectroscopy suggest that the A21G (A73G in tRNA) exchange results in a decrease of melting transition cooperativity and a destabilization of the terminal G1–C20 (G1–C72 in tRNA) base pair. Furthermore, the fact that this 3′-terminal imino proton is more solvent-exposed at physiological temperature might be another indication for the importance of the stability of the terminal base pair for specific tRNA recognition.

INTRODUCTION

Fidelity of protein biosynthesis depends on the specific recognition between tRNAs and their cognate aminoacyl-tRNA synthetases (aaRS), which esterify the tRNA with the correct amino acid. The 20 different aaRS are divided into two classes, each consisting of 10 members, on the basis of the ATP-binding motifs. The members of class I share one common 3-D structural domain with the characteristic signatures HIGH and KMSK associated with the Rossman fold. The 10 other enzymes form the group of class II aaRS, which share one or more of three structural motifs (1).

The structural and sequence elements of the tRNA required for the recognition process are called identity elements. They are located in at least two regions of the tRNA– (i) in the discriminator base position 73 and (ii) in the acceptor stem and/or in the anticodon loop and less frequently in the variable pocket or in the extra arm (2–8). The special role of the discriminator base is indicated by the finding that virtually all tRNAs in any family and most tRNAs which accept chemically similar amino acids have the same residue at position 73 (9). It is the only variable unpaired nucleotide near the aminoacylation site, except for $tRNA^{His}$ in archaebacteria, eubacteria or yeast mitochondria (10). We have shown before that the discriminator base plays a central and important role in the recognition of all human tRNAs with a long extra arm (class II tRNAs) by their cognate aaRS. The exchange of the discriminator base A73 for G is alone sufficient to convert human $tRNA^{Leu}$ into a serine-acceptor *in vitro* (11). The reverse experiment, the exchange of G73 in human $tRNA^{Ser}$ for the $tRNA^{Leu}$ specific A, and to C or U causes a total loss of serine acceptance without creating any leucine acceptance (12). These results suggest (i) that the discriminator base G73 is essential for recognition by human SerRS and (ii) that the discriminator base A73 of human $tRNA^{Leu}$ alone protects this tRNA against serylation by SerRS. We show here that the discriminator base is not only important for the recognition process, but also for the dynamic structure of the tRNA.

There are several possible reasons for the importance of the discriminator base in aaRS recognition of tRNAs. The discriminator base could be a site of direct contact for the aaRS.

*To whom correspondence should be addressed. Tel: +49 921 553540; Fax: +49 921 553544; Email: paul.roesch@uni-bayreuth.de

[+]Present address: Department of Biochemistry, Faculty of Medicine, Technion-Israel, Haifa 31096, Israel

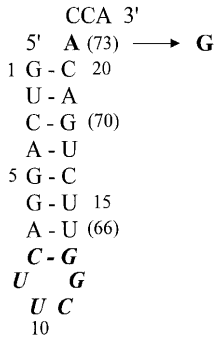

Figure 1. Sequence of the microhelices (acceptor stem of human tRNA^{Leu}) with A or G (printed in bold) in the discriminator base position 21. The additional C–G pair and stable tetraloop is printed in italics. Numbers in brackets identify positions in complete tRNA^{Leu}.

Examples of this are seen in the crystal structures of the yeast AspRS–tRNA^{Asp} and *Thermus thermophilus* SerRS–tRNA^{Ser} complexes (13–15). Alternatively or additionally, the discriminator base could influence the structure at the end of the acceptor stem and thereby its interaction with aaRS or other proteins (16). An example of this is seen in the crystal structure of the *Escherichia coli* GlnRS–tRNA^{Gln} complex, in which the discriminator base G73 facilitates the melting of the U1–A72 base pair of tRNA^{Gln} and bending of the CCA end for it to fit into the catalytic pocket of GlnRS (17,18).

Chemical and structural studies on tRNA acceptor stem microhelices have been used recently to study the effect of discriminator base on tRNA acceptor stem structure. These studies with tRNAs and tRNA microhelices corresponding to mutant *E.coli* initiator tRNA and *E.coli* tRNA^{Ala} have shown that the nature of the discriminator base can influence tRNA structure at the end of the acceptor stem (16,19,20).

The above studies were carried out with tRNA and tRNA microhelix variants in which the position corresponding to the discriminator base was changed from A to C or U. In view of the critical role of G73 in tRNA^{Ser} for its aminoacylation by human SerRS and the critical role of A73 in human tRNA^{Leu} for blocking its misaminoacylation by SerRS, it was of interest to compare the structure of two tRNA acceptor stems which differed only in having either A or G at the discriminator position. Here, we describe the use of NMR and UV melting studies on tRNA^{Leu} acceptor stem microhelices containing either A or G at the position corresponding to the discriminator base in tRNA. We show that change of A to G at the discriminator position substantially destabilizes the neighbouring G–C base pair. We suggest that this propensity of the G–C base pair to melt could be important in recognition of tRNA^{Ser} by human SerRS.

MATERIALS AND METHODS

RNA synthesis and purification

The sequences coding for the two microhelices including the T7 promoter were cloned in pUC19. *Escherichia coli* JM109 was used as a host for propagation of the two plasmids. The plasmids were linearized with *Bst*NI and the microhelices were transcribed in milligram quantities by using T7 RNA polymerase (21). The reaction was primed by GMP and the product was purified by electrophoresis on 20% denaturing polyacrylamide gels.

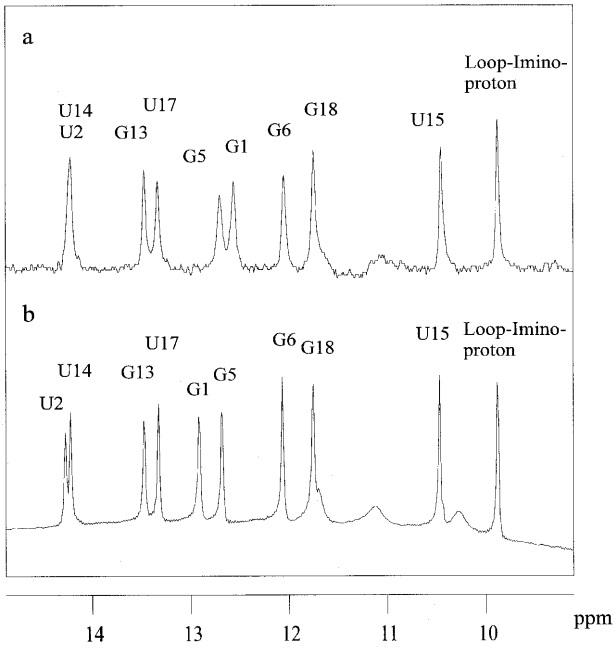

Figure 2. Imino proton region of 1D NMR spectra of A21 (**a**) and G21 (**b**) variants in 10 mM potassium phosphate, pH 6.4, 50 mM NaCl. All base paired imino protons are labelled.

Homogeneity of the 5′- and 3′-end was verified in pilot reactions by mobility shift analyses of the 5′- and 3′-^{32}P-labelled microhelices, respectively (22). Purified RNA was dialysed against H_2O and lyophilized.

NMR spectroscopy

NMR spectra were recorded on a Bruker AMX-400 or AMX-600 NMR spectrometer operating at proton frequencies of 400 and 600 MHz, respectively. Homonuclear one- and two-dimensional (2D) NMR spectra were recorded at 0.5–1.5 mM RNA concentration in 10 mM potassium phosphate buffer, pH 6.4, 50 mM NaCl. To investigate temperature effects on the RNA spectra, 2D experiments were performed at 4, 25 and 40°C. All 2D NMR spectra were recorded in the phase-sensitive mode using the TPPI method (23).

One-dimensional (1D) spectra and 2D nuclear Overhauser enhancement (NOE) experiments in H_2O for the assignment of exchangeable protons were acquired using the 1331 solvent suppression scheme (24). Assignments for the non-exchangeable proton resonances were derived from 2D NOE spectra (NOESY, 25), double-quantum filtered correlated spectra (DQF-COSY, 26), and total correlated spectra with suppression of NOESY-type cross peaks (Clean-TOCSY, 27) experiments. Mixing times were 80 ms for TOCSY and 60, 100, 200 and 400 ms for NOESY experiments.

Thermodynamic analysis

Equilibrium melting curves were obtained using a Hewlett-Packard 8452 diode array spectrophotometer equipped with a Pelletier element and a temperature sensor inserted into a 1 cm cell. Before each measurement the RNA (2 µM) was renatured by heating to 90°C for 3 min, followed by slow cooling to room temperature in 10 mM potassium phosphate, 50 mM NaCl, pH 6.4 buffer.

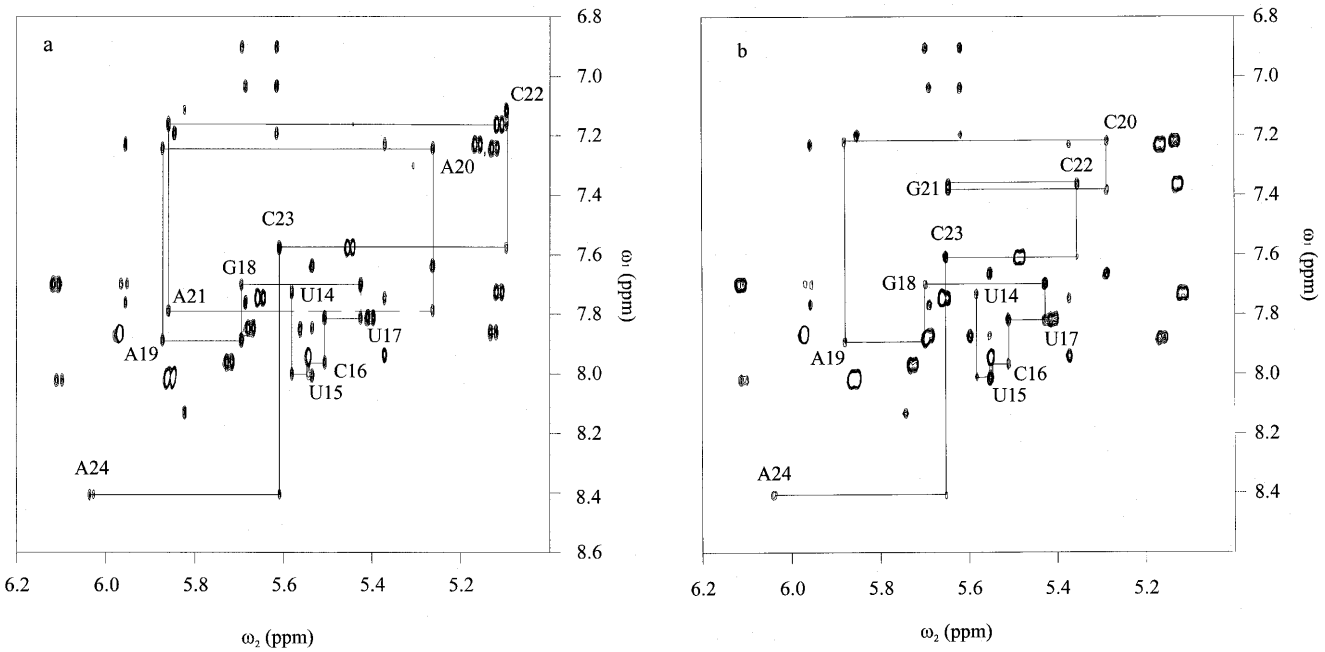

Figure 3. Fingerprint (aromatic to anomeric) regions of 400 ms NOESYs acquired at 25°C of A21 (**a**) and G21 variant (**b**). Each H8/H6(i)–H1′(i)–H8/H6(i+1) walk is shown in solid lines. The labelled cross peaks correspond to the intranucleotide H8/H6–H1′ NOEs.

Samples were heated at a rate of 0.5°C/min. Spectra from 234 to 350 nm were recorded at 1°C intervals. Reversibility of the melting process was examined by cooling to the initial temperature. Thermal denaturation curves were followed by the increase of absorbance at 260 nm. The thermodynamic parameters were determined on the basis of the two-state model from the temperature dependence of the equilibrium constant (28).

RESULTS

Design of the tRNA microhelices with different nucleotides at the discriminator position 21

To investigate conformational properties of two tRNAs differing only at the discriminator base we synthesized two microhelices, one with the A21, the other one with G21, comprising the acceptor stem of $tRNA^{Leu}$ (Fig. 1). The two strands of the stem were extended by an additional C–G base pair in order to mimic the structural stability of the mature domain and were connected by the structurally well-characterized UUCG tetraloop (29). These two microhelices are no substrates for aminoacylation with LeuRS and SerRS, respectively. Aminoacylation was performed as described by Breitschopf and Gross (11) with 15 µM microhelix RNA and 15 µM [^{3}H]serine (1.04 TBq/mmol) for serylation or 10 µM microhelix RNA and 10 µM [^{3}H]leucine (2.15 TBq/mmol) for leucylation.

Imino proton spectra of the microhelices

The imino proton region of the two microhelices at 25°C (Fig. 2a and b) could be assigned using 2D NOE experiments. As expected, the imino proton spectra of the microhelices exhibit sharp signals originating from the 8 bp in the stem (Fig. 1) and from a U–G-base pair within the UUCG-loop (29). The two spectra are nearly identical except for noticable differences in imino proton chemical shifts of G1 and U2 for the two variants. These imino protons are involved in the two 3′-terminal base pairs. The G1 imino proton of the G1–C20 base pair of the wild-type microhelix resonates 0.3 p.p.m. upfield of the terminal base pair of the mutant microhelix with G at the position of the discriminator base. A similar but less pronounced effect could be observed for the imino proton of the U2–A19 base pair with an upfield chemical shift of ~0.1 p.p.m.

Upfield shifts for imino protons in base pairs are induced by base ring currents of the regularly stacked nearest-neighbour base pairs (30) and may be an indicator for improved base stacking. Thus, the observed chemical shift differences of the two terminal base pairs are initial indications for possible differences in stacking geometries at the 3′-end of the two microhelices caused by different discriminator bases.

2D NMR spectroscopy

To assign the non-exchangeable protons of the microhelices, previously reported methods and assignment strategies were used (31,32). Following these procedures all base protons, H1′, H2′ and several of H3′, H4′, H5′/H5″ could be assigned for both molecules (Fig. 3a and b). Each portion of this NOESY spectrum contains NOE cross peaks between H1′/H5 (5.0–6.2 p.p.m.) and H8/H6/H2 (6.8–8.2 p.p.m.) resonances. H8/H6(i)–H1′(i)–H8/H6(i+1) connectivities at a long mixing time provided information about A-form stacking. The set of internucleotide NOE connectivities demonstrates that both microhelices adopt helical conformation at their respective 3′-ends. This was confirmed by an alternative assignment pathway using H8/H6(i)–H2′(i)–H8/H6(i+1) connectivities. For an A-form helix with C3′-*endo* sugar pucker, the coupling constant between the sugar protons H1′ and H2′ ($J_{1'2'}$) is typically <2 Hz and thus smaller than the line-width. H1′–H2′ couplings are therefore not seen in the DQF-COSY spectrum for the stem protons of either microhelix. The absence of those cross-peaks between the ribose protons in each stem also confirms the A-helical nature of the stem of both molecules.

Comparison of the NOE pattern at the 3′-end of the microhelices

The two microhelices exhibit overall identical conformation at their 3′-ends. The wild-type microhelix and the G21 variant maintain the stacked conformation throughout the 3′-CCA end. The stacking is independent of the presence of A or G at position 21. Internucleotide NOEs are observed from U14 to A24 for both microhelices in the fingerprint region of the 400 ms NOESY spectrum (Fig. 3a and b). The same result was obtained for the alternative H8/H6 to H2′ connectivities which confirmed that both microhelices exhibit A-form stacking from position 14 to 24. Especially for the wild-type microhelix A-form typical NOEs could be observed. The H2 proton of the discriminator base A21 shows strong NOEs to the H1′ protons of G1 and C22 (Fig. 3b). Such NOEs can only be observed if A21 is involved in A-form stacking. H1′–H2′ cross peaks could be detected in the DQF-COSY spectrum for only two loop riboses and for C23 and A24, the probable reason being C2′-*endo* conformation of these sugars. This could be due to flexibility of the two terminal nucleotides at the 3′-end. As these features are common to both molecules, they further indicate the two microhelices to exhibit the same overall conformation. Additionally, no long range NOEs from the 3′- to the 5′-end could be observed for either variant, even at long mixing times. Such NOEs would be typical for fold back structures, where the two termini are close. In order to study the temperature dependence of the common NOE pattern, we performed the same NMR experiments at 4, 15 and 40°C. The measurements indicate that the conformations at the 3′-end are not affected by temperature changes. From all these results we conclude that the wild-type microhelix exhibits the same overall conformation at the 3′-end as the G21 variant under the conditions used here.

Chemical shift analysis of the protons of the nucleotides located at the 3′-end

In order to further investigate the effect of the discriminator base on the structure at the 3′-end we compared the chemical shift of the aromatic H8/H6 and of the sugar H1′ protons at the 3′-end (nt 17–24) for both variants at 25°C (Fig. 4). Chemical shift changes (Δδ values) on A21G substitution do not exceed 0.01 p.p.m. for the aromatic and sugar protons of nt 17–19 within the stem and the 3′-terminal A24. The H1′ proton of C22, the nucleotide in the 3′-neighbourhood of the discriminator base, undergoes, however, a chemical shift change of nearly 0.3 p.p.m. downfield on A21G substitution. Δδ-values of the aromatic H8/H6 protons yielded a maximum value of +0.2 p.p.m. as observed for the C22 H6 proton. The Δδ-value of the aromatic protons roughly indicate the stacking properties of the two variants (33). The chemical shift of these protons reflects the extent of nucleotide shielding that is dependent on the stacking in a helix. An upfield shift indicates better stacking properties. Thus, the Δδ value of +0.2 p.p.m. for the C22 H6 proton and the Δδ value of +0.03 p.p.m. for the C23 H6 proton might suggest better stacking properties of the 3′-ACCA compared to the 3′-end of the G21 variant. The two microhelices exhibit the same NOE pattern suggesting identical overall conformation at the 3′-end, upfield shifts of H1′ and H6 proton resonances of C22 and C23 might suggest improved stacking of the 3′-end of wild-type A21 variant in comparison to the G21 microhelix.

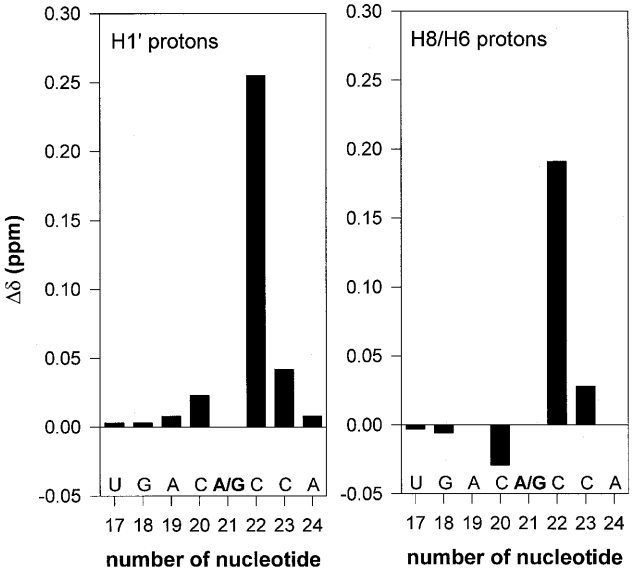

Figure 4. Differences between chemical shifts (Δδ) of the H1′ and H8/H6 protons between the G21 and the A21 variant at 25°C. Shown are the chemical shift differences from nucleotides located at the 3′-end of the microhelices.

UV melting studies

To characterize the overall stability of the microhelices, UV melting curves were recorded (Fig. 5). The thermodynamic parameters melting temperature (T_m) and van't Hoff enthalpy of the duplex formation (ΔH^0) were determined by fitting the melting curve data to a two-state, unimolecular model (27). Data evaluation yielded $T_m = 74.4 \pm 0.1$°C for the A21 variant and $T_m = 74.5 \pm 0.1$°C for the G21 variant. The T_m values are almost identical as all nucleotides involved in base pairing are identical in both microhelices. This result is in good agreement to our NMR data obtained from NOE experiments suggesting the same overall conformation for both molecules. Surprisingly, the experimental ΔH^0 values are significantly different. Alteration of the discriminator base from A to G reduces the ΔH^0 value from 42.3 ± 2.0 to 36.3 ± 2.0 kJ/mol. Thus, incorporation of G at position 21 in the microhelix reduces cooperativity of the melting transition. For the G-variant, base pairs in the stem might be of grossly varying stability, possibly in contrast to the wild-type RNA, where a higher cooperativity of the transition could be observed. The different melting behaviour may also explain the differences of the proton chemical shifts of the nucleotides located at each microhelix 3′-end. The higher cooperativity of transition could result from better stacking properties of the A21 variant 3′-end as proposed from the NMR experiments.

Temperature dependence of the imino protons

To gain more insight into the nature of base pair stability of the microhelices, we performed temperature-dependent 1D NMR experiments of the base paired imino protons. The spectra reveal further differences for the two variants. Interestingly, at 40°C the G1–C20 imino proton signal of the G21-variant is broader and exhibits a poorer signal to noise ratio compared to other imino proton signals within the same molecule (Fig. 6). This is due to a faster exchange of this labile proton with water molecules.

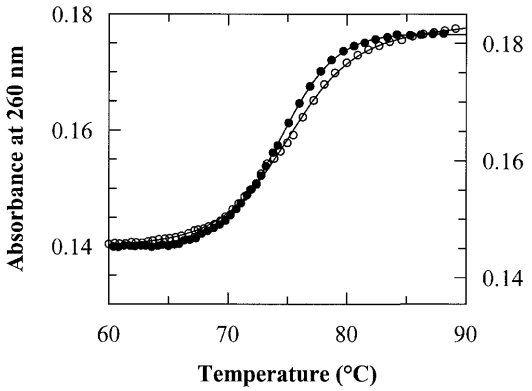

Figure 5. Melting curves of A21 variant (●, left scale) and the G21 variant (○, right scale) as monitored by the absorbance at 260 nm. Measurements were made in 10 mM potassium phosphate, 50 mM NaCl, pH 6.4. The microhelix concentrations were 2 µM.

Thus, at physiological temperature the G1 imino proton is much more solvent exposed compared to others in the same molecule. In contrast, the G1–C20 resonance of the wild-type microhelix remains narrow at this temperature and exhibits a signal to noise ratio virtually identical to that of the other imino protons. Thus, the terminal base pair of the wild-type microhelix seems to be more rigid than that of the G21 variant. The broadening of specific signals occurs over a temperature range from 40 to 55°C for the mutant microhelix, whereas most of the signals of the A21 wild-type broaden at or above 50°C, confirming the UV melting studies.

DISCUSSION

Structural analysis of wild-type and variant forms of human tRNA^{Leu} acceptor stem microhelices

Our results obtained from NMR and UV-melting studies suggest that the nature of the discriminator base in human tRNA^{Leu} microhelices influences the stability of the terminal G1–C20 base pair. For *E.coli* tRNA^{Ala}, it has been shown that the thermodynamic parameters of acceptor stem microhelices are dependent on the nature of the discriminator base (19). An A at the discriminator position contributes maximally to the duplex stability. This is in good agreement with our results obtained for human tRNA^{Leu} microhelices, where the variant with the natural discriminator base A21 has a more stable G1–C20 base pair in comparison to the G21 variant. Thus, since this exchange of the discriminator base totally switches the acceptor specificity from Leu to Ser, the stability of the terminal base pair may be very important for the specific recognition of tRNA by LeuRS and by SerRS (see below).

NOE experiments of both human tRNA^{Leu} microhelices indicate that they have the same overall conformation. The only differences observed from UV-melting studies and temperature-dependent 1D NMR experiments are the cooperativity of the melting transition and the stability of the terminal base pair. The wild-type tRNA^{Leu} microhelix has an A at position 21, the discriminator base. Such molecules with the 3′-ACCA sequence continue the A-form stacking of the acceptor stem as seen in the X-ray structure of yeast tRNA^{Phe} (34,35) and in the NMR structure of a *E.coli* tRNA^{Ala} microhelix (36) agreeing with our NMR data for the A21 variant. The NOESY spectra exhibit the

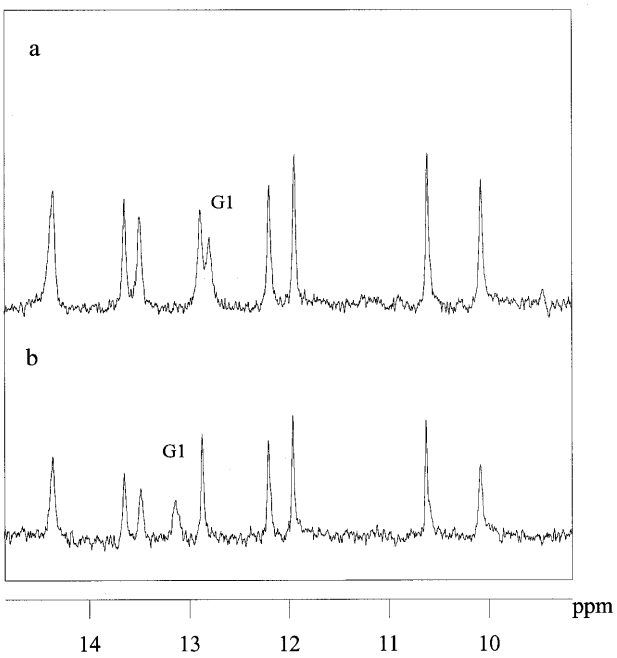

Figure 6. Iminoproton spectrum of of the A21 variant (**a**) and the G21 (**b**) variant at 40°C. The spectra were recorded in 10 mM potassium phosphate, pH 6.4, 50 mM NaCl. The imino proton of the G1–C20 base pair is labelled.

typical NOE pattern observed for A-helix geometries from U14 within the acceptor stem to the 3′-A24. The same result was obtained for the G21 variant. Thus, the A-type stacking from U14 to A24 is a common feature for the 3′-strand in both molecules and the data suggest no different populations of conformers in the two variants.

This is in contrast to NMR studies of mutant forms of *E.coli* initiator methionyl-tRNA acceptor stem microhelices (20). The 3′-ACCA sequence of the wild-type A19 variant extends the stacking of the acceptor stem as seen here but in the U19 variant the 3′-end folds back towards the 5′-end. The exchange of a purine for a pyrimidine leads probably to more possible conformational rearrangements compared to a purine-purine exchange in the tRNA^{Leu} system. A comparison of available tRNA sequences shows that the discriminator base is preferentially occupied by a purine (37) and X-ray structures of different tRNAs carrying a purine at the position 73 do not exhibit a fold-back structure (38).

Role of the discriminator base in recognition of tRNAs by human SerRS and LeuRS

Recognition by human SerRS. We showed previously that mutation of G73 in human tRNA^{Ser} to A, C or U abolished aminoacylation of the tRNA by SerRS (11). In addition, mutation of A73 to G73 in human tRNA^{Leu} converted it into a serine acceptor. Thus, G73 at the discriminator position is critical for recognition of tRNAs by human SerRS. It is possible that human SerRS makes direct contact with G73 and that this contact is critical for the CCA end of the tRNA to fit into the catalytic pocket of the enzyme. The crystal structure of *Tth* SerRS–tRNA^{Ser} complex shows that SerRS interacts directly with G73 through an ionic hydrogen bond between the Glu278 of the enzyme and the 2-N group of G73. Alternatively or additionally, the destabilisation of the G1–C72 base pair by the discriminator base G73 (see above)

means that human SerRS could melt the base pair and that melting of the base pair is essential for the CCA end of the tRNA to fit into the catalytic pocket of the enzyme.

The importance of G73 for aminoacylation of human $tRNA^{Ser}$ is reminiscent of the importance of G73 in *E.coli* $tRNA^{Gln}$ and in yeast $tRNA^{Asp}$ for their recognition by the corresponding aaRS. In the crystal structure of the *E.coli* GlnRS–$tRNA^{Gln}$ complex, the U1–A72 base pair of the tRNA is broken and the GCCA extension of the acceptor stem is bent towards the catalytic pocket of GlnRS (17,18). These structural changes result in a conformation that is stabilized by base-specific intramolecular hydrogen bond between the discriminator base G73 and phosphate 72. Thus, presence of G73 at the discriminator position facilitates melting of the U1–A72 base pair that is necessary for the CCA end of the $tRNA^{Gln}$ to fit into the catalytic pocket of GlnRS.

The propensity of a base pair to be disrupted does not, however, mean that it will always be disrupted by a protein. Yeast $tRNA^{Asp}$ has the same U1–A72 base pair and G73 at the discriminator position as *E.coli* $tRNA^{Gln}$. However in the yeast AspRS–$tRNA^{Asp}$ complex, the U1–A72 base pair is not disrupted and the AspRS makes base specific contacts with the U1–A72 base pair and with G73 (13,14).

Recognition of $tRNA^{Leu}$ by human LeuRS. The discriminator base A73 is also important for recognition of the tRNA by human LeuRS. Mutation of A73 to G73 or C73 abolished aminoacylation of the tRNA with leucine, and mutation to U73 greatly reduced leucine acceptor activity (12). Our finding that the $tRNA^{Leu}$ microhelix with A21 (corresponding to the discriminator base 73) has a stable RNA A helical structure in which the 3′-terminal ACCA sequence extends the stacking of the acceptor stem suggests that the rigidity of the acceptor stem could be important for recognition of $tRNA^{Leu}$ by human LeuRS. One possibility is that the rigidity of the acceptor stem positions the CCA end in the correct spatial location with respect to the remainder of the identity elements in the human $tRNA^{Leu}$ (for example the long variable loop and stem, also see 36). Another possibility is that the enzyme also contacts A73 directly.

ACKNOWLEDGEMENTS

We thank Thomas Schindler for help with the UV melting curves and Dr Heinrich Sticht for valuable discussion. M.H., K.B. and H.J.G. have been supported by Deutsche Forschungs-gemeinschaft, SFB 165 and by Fonds der Chemischen Industrie, A.U.M. received a fellowship from the Graduiertenkolleg ‘Biosynthese der Proteine und Regulation ihrer Aktivität’ and U.L.R. is supported by grant GM17151 from National Institutes of Health.

REFERENCES

1 Eriani, G., Delarue, M., Poch, O., Gangloff, J. and Moras, D. (1990) *Nature*, **347**, 203.
2 Normanly, J. and Abelson, J. (1989) *Annu. Rev. Biochem.*, **58**, 1029–1049.
3 Schimmel, P. (1989) *Biochemistry*, **28**, 2747–2759.
4 Schulman, L.H. (1991) *Prog. Nucleic Acid Res. Mol. Biol.*, **41**, 23–87.
5 Giegé, R., Puglisi, J.D. and Florentz, C. (1993) *Prog. Nucleic Acid Res. Mol. Biol.*, **45**, 129–206.
6 McClain, W.H. (1993) *J. Mol. Biol.*, **234**, 257–280.
7 McClain, W.H. (1993) *FASEB J.*, **7**, 72–77.
8 Saks, M.E., Sampson, J.R. and Abelson, J.N. (1994) *Science*, **263**, 191–197.
9 Crothers, D.M., Seno, T. and Söll, D. (1972) *Proc. Natl. Acad. Sci. USA*, **69**, 3063–3067.
10 Steinberg, S., Misch, A. and Sprinzl, M. (1993) *Nucleic Acids Res.*, **21**, 3011–3015.
11 Breitschopf, K. and Gross, H.J. (1994) *EMBO J.*, **13**, 3166–3169.
12 Breitschopf, K. and Gross, H.J. (1996) *Nucleic Acids Res.*, **24**, 405–410.
13 Cavarelli, J., Ress, B., Ruff, M., Thierry, J.-C. and Moras, D. (1993) *Nature*, **362**, 181–184.
14 Ruff, M., Krishnaswamy, S., Boeglin, M., Poterszman, A., Mitschler, A., Podjarny, A., Rees, B., Thierry, J.C. and Moras, D. (1991) *Science*, **252**, 1682–1689.
15 Cusack, S., Yaremchuk, A. and Tukalo, M. (1996) *EMBO J.*, **15**, 2834–2842.
16 Lee, C.P., Mandal, N., Dyson, M.R. and RajBhandary, U.L. (1993) *Proc. Natl. Acad. Sci. USA*, **90**, 7149–7152.
17 Sherman, J.M. and Söll, D. (1996) *Biochemistry*, **35**, 601–607.
18 Rould, M.A., Perona, J.J., Söll, D. and Steitz, T.A. (1989) *Science*, **246**, 1135–1141.
19 Limmer, S., Hoffmann, H.-P., Ott, G. and Sprinzl, M. (1993) *Proc. Natl. Acad. Sci. USA*, **90**, 6199–6202.
20 Puglisi, E.V., Puglisi, J.D., Williamson, J.R. and RajBhandary, U.L. (1994) *Proc. Natl. Acad. Sci. USA*, **91**, 11467–11471.
21 Zawadzki, V. and Gross, H.J. (1991) *Nucleic Acids Res.*, **19**, 1948.
22 Beier, H. and Gross, H.J. (1991) In Brown, T.A. (ed.), *Essential Molecular Biology, A Practical Approach*. Vol. II, IRL Press Oxford, New York, Tokyo, pp. 221–236.
23 Marion, D. and Wüthrich, K. (1983) *Biochem. Biophys. Res. Commun.*, **113**, 967–974.
24 Hore, P.J. (1983) *J. Magnet. Reson.*, **55**, 283–300.
25 Bodenhausen, G., Kogler, H. and Ernst, R.R. (1984) *J. Magnet. Reson.*, **58**, 370–388.
26 Rance, M., Sorensen, O.W., Bodenhausen, G., Wagner, G., Ernst, R.R. and Wüthrich, K. (1983) *Biochem. Biophys. Res. Commun.*, **117**, 470–485.
27 Griessinger, C., Otting, G., Wüthrich, K. and Ernst, R.R. (1988) *J. Am. Chem. Soc.*, **110**, 7870–7872.
28 Puglisi, J.D. and Tinoco, I., Jr (1989) *Methods Enzymol.*, **180**, 304–325.
29 Allain, F.H.T. and Varani, G. (1995) *J. Mol. Biol.*, **250**, 333–353.
30 Giessner-Prettre, C. and Pullman, B. (1976) *Biochem. Biophys. Res. Commun.*, **70**, 578–581.
31 Varani, G. and Tinoco, I., Jr (1989) *Q. Rev. Biophys.*, **24**, 479–532.
32 Varani, G., Aboul-ela, F. and Allain, F.H.T. (1996) *Prog. Nuclear Magnet. Reson. Spectr.*, **29**, 51–127.
33 Hader, P.A., Alkema, D., Bell, R.A. and Neilson, T. (1982) *J. Chem. Soc. Chem. Commun.*, **1**, 10–12.
34 Ladner, J.E., Jack, A., Robertus, J.D., Brown, R.S., Rhodes, D., Clark, B.F. and Klug, A. (1975) *Proc. Natl. Acad. Sci. USA*, **72**, 4414–4418.
35 Suddath, F.L., Quigley, G.J., McPherson, A., Sneden, D., Kim, J.J., Kim, S.H. and Rich, A. (1974) *Nature*, **248**, 20–24.
36 Ramos, A. and Varani, G. (1997) *Nucleic Acids Res.*, **25**, 2083–2090.
37 Sprinzl, M., Dank, N., Nock, S. and Schön, A. (1991) *Nucleic Acids Res.*, **19**, 2127–2171.
38 Saenger, W. (1984) *Principles of Nucleic Acid Structure*. Press Springer, New York.